

*This study considers a high-speed permanent magnet motor designed to drive unmanned aerial vehicles and ground robotic systems. The scientific-practical task addressed is to establish a quantitative relationship between the components of electromagnetic losses and the thermal state of the motor in a wide range of operating modes (5000–23000 rpm, 1–54 A).*

*A multiphysics numerical field mathematical model of a small-sized high-speed permanent magnet motor operating as part of an unmanned aerial vehicle has been constructed. The model resolves a coupled electromagnetic-thermal problem refining the temperature field distribution and parameters of active materials: the dependence of the residual magnetic induction of permanent magnets.*

*It was found that the distribution of specific losses in the cross section is deeply uneven: the maximum values are concentrated at the edges of the stator teeth and exceed the losses in the permanent magnets and yoke by 1.5–2.5 orders of magnitude. The distribution of the thermal field with increasing current was established: at  $I \leq 14$  A, magnetic losses prevail, and at  $I > 27$  A, losses in the winding become predominant and reach 201 W at a current of 54 A. This is 2.5–3.5 times more than magnetic losses. With increasing current, the loss curves for different speeds gradually coincide: at  $I = 54$  A, the difference between 5000 and 23000 rpm is only  $\approx 20$  W ( $\approx 7\%$  of the total losses of 260–280 W).*

*At speeds above 17,000 rpm, the temperature of permanent magnets exceeds  $80^\circ\text{C}$ , the residual induction decreases by 6–8% of the rated value, which leads to a decrease in the electromagnetic torque by 3–4%. A critical value of the average motor heating has been established, at which the risk of irreversible demagnetization of magnets occurs, which corresponds to  $\approx 216^\circ\text{C}$ , at a speed of  $n > 11,000$  rpm and at maximum current.*

*The results could be used to optimize high-speed motors with permanent magnets*

*Keywords: high-speed motor, losses in the magnetic core, multiphysics model, thermal state*

# DETERMINING THE EFFECT OF ACTIVE LOSSES ON THE THERMAL STATE OF A HIGH-SPEED PERMANENT MAGNET MOTOR

**Mykhailo Kovalenko**

*Corresponding author*

Candidate of Technical Sciences, Associate Professor\*

E-mail: kovalenko87ma@gmail.com

ORCID: <https://orcid.org/0000-0002-5602-2001>

**Yurii Haidenko**

Candidate of Technical Sciences, Associate Professor\*

ORCID: <https://orcid.org/0000-0001-5862-2812>

**Serhii Tsyvinskyi**

Candidate of Technical Sciences, Associate Professor\*

ORCID: <https://orcid.org/0000-0002-2800-6709>

**Oleksandr Semeniuk**

PhD Student\*

ORCID: <https://orcid.org/0009-0005-9959-4041>

**Oleh Bazarov**

PhD Student\*

ORCID: <https://orcid.org/0009-0008-8491-2678>

\*Department of Electromechanics

National Technical University of Ukraine

«Igor Sikorsky Kyiv Polytechnic Institute»

Peremohy ave., 37, Kyiv, Ukraine, 03056

Received 12.03.2026

Received in revised form 25.05.2026

Accepted 03.06.2026

Published 23.06.2026

**How to Cite:** Kovalenko, M., Haidenko, Y., Tsyvinskyi, S., Semeniuk, O., Bazarov, O. (2026).

Determining the effect of active losses on the thermal state of a high-speed permanent magnet motor. *Eastern-European Journal of Enterprise Technologies*, 3 (5 (141)), 17–25.

<https://doi.org/10.15587/1729-4061.2026.364568>

## 1. Introduction

The evolution of energy, electric transport, and aviation technology is characterized by the use of compact, highly efficient drive motors with high specific power. Due to their high specific power, compactness, and energy efficiency, high-speed permanent magnet motors (HPPMs) are increasingly replacing asynchronous motors in the above-mentioned areas. Compact dimensions and high specific power are achieved through the use of available drive controllers that allow a significant increase in the HPPM supply frequency. However, a further increase in the supply frequency, rotation speed, and specific power leads to significant heat generation in a limited volume of the machine. The thermal state of the motor, especially with permanent magnets, is a resulting factor that determines not only energy performance but also the reliability of the system under various (especially emergency) modes.

With increasing rotation speed, electromagnetic losses in active structural elements, mechanical losses, and eddy currents in permanent magnets increase [1]. In HPPMs above 10,000 rpm, specific losses reach 25–80 W/cm<sup>3</sup>. Excessive heating of permanent magnets leads to local overheating and the risk of their demagnetization.

For aviation, where HPPMs are used as drive motors, determining the temperature state is a matter of flight safety and reliability because overheating can cause demagnetization of magnets, it accelerates thermal aging of insulation, or leads to thermal breakdown of winding insulation. In electric transport, determining the impact of losses on the thermal state makes it possible to define energy-efficient modes, which allows for the maximum use of motor potential without the risk of its sudden failure. In addition, optimization of thermal processes makes it possible to reduce the power of cooling systems, improve weight-dimensional indicators,

as well as improve the reliability of the converter, which is important for vehicles and aviation equipment.

In actual HPPMs, the nature of the thermal field distribution in active materials is significantly heterogeneous because magnetic losses are distributed unevenly in different structural areas of the magnetic core.

The relevance of research into the thermal processes in HPPMs is due to the need to take into account the uneven distribution of active losses depending on the thermal state when designing new generation electric machines. The nature of relationship between losses and thermal state is a necessary condition for designing reliable, compact, and energy-efficient drives for modern industrial and transportation systems.

---

## 2. Literature review and problem statement

---

An analysis of losses and thermal state of a powerful high-speed synchronous motor with permanent magnets was performed in [2]. An improved method for calculating losses in the magnetic core was proposed, taking into account higher harmonics of the field, which makes it possible to increase the accuracy of estimating losses at high rotation speeds. The analysis of temperature and heating was performed by the method of hydrodynamics considering cooling. However, the work did not pay enough attention to the effect of temperature on the magnetic properties of materials and on the accuracy of calculating losses.

In study [3], a methodology for calculating losses and thermal state of the rotor of a high-speed motor with a capacity of 100 kW at a speed of 32,000 rpm was proposed. The analysis focused on calculating mechanical losses, which are significantly manifested at high rotation speeds. The authors proposed an empirical calculation for estimating losses taking into account the roughness of the rotor surface and flow turbulence. The disadvantage of the work is the lack of experimental verification of the modeling results.

That study was advanced in [4], in which the calculation of losses and thermal analysis of HPPM made with an amorphous alloy stator and built-in permanent magnets was performed. The authors use an interconnected electromagnetic-thermal calculation to determine the temperature distribution. It is shown that the use of an amorphous alloy makes it possible to reduce losses in the magnetic core by 60–70% compared to classical electrical steel. However, the work does not consider the influence of vibrations and acoustic noise on the thermal state of the motor.

In [5], a HPPM with a rated speed of 90,000 rpm was investigated. The authors proposed an algorithm for calculating the magnetic and thermal fields to obtain an accurate temperature distribution, taking into account its influence on the electromagnetic properties of materials. It is shown that at this speed of rotation, mechanical losses account for the largest share of the total losses. The modeling results were verified experimentally, and the error is no more than 2–3°C. The model does not take into account the resource of the insulating materials of the windings.

In [6], a three-dimensional numerical model is described for assessing the thermal state of high-speed motors. A feature of the model built is the increased calculation accuracy, which reduces the temperature calculation error by 8–12%. The influence of the dependence of loss coefficients on temperature on the calculation accuracy was also analyzed and an optimal

methodology for choosing the iteration step was proposed. However, the study does not take into account the influence of slot and interturn insulation on the calculation result.

Paper [7] reports modeling electromagnetic losses and analyzing the effect of demagnetization for HPPM. The authors proposed methods for reducing rotor eddy currents by optimizing the configuration of the stator slots and performing additional slots on the rotor. The operational factors under which irreversible demagnetization of permanent magnets occurs are analyzed. The disadvantage of the study is the lack of analysis of the effect of harmonics from the inverter on losses.

Another approach is proposed in [8], in which the design of a rotor with solid permanent magnets is considered, in order to reduce eddy currents. The authors proposed a methodology for optimizing the rotor winding taking into account the requirements of mechanical strength and reducing losses. Thermal analysis was implemented using the finite element method taking into account the uneven distribution of losses. However, the work did not investigate the effect of thermal conductivity of insulating materials on the temperature regime of motor operation.

The assessment of various cooling techniques on thermal state was carried out in [9]. The work systematized approaches to calculating various components of losses, including in the magnetic core, winding, as well as mechanical losses, which is important for assessing the thermal state. However, the review does not contain a comparative analysis of the economic efficiency of different approaches to taking into account the thermal regime.

In study [10], a comparative analysis of heat transfer characteristics for different cooling systems of a 120 kW HPPM was carried out. The authors proposed a methodology for optimizing the geometry of cooling channels to increase the heat transfer coefficient. It has been shown that this cooling system provides 25–30% more efficient heat removal compared to conventional systems. However, the authors did not consider the effect of harmonics on heating.

That issue was further advanced in [11], in which the influence of power harmonics on losses and heating of HPPM is investigated. The authors proposed an approach based on the equivalent current layer for calculating eddy currents. Comparison of the calculation results with the data obtained by the finite element method shows satisfactory convergence. As a result, it is shown that increasing the number of slots per pole makes it possible to reduce eddy currents by 15–20%. The disadvantage of the work is the lack of analysis of the influence of power harmonics on the insulation resource and its heating.

In work [12], a thermal analysis of a 37.5 kW motor at a speed of 30,000 rpm was carried out. The authors used the method of thermal and hydrodynamic analysis for a comprehensive assessment of the condition of the motor. It is shown that the use of an amorphous alloy instead of electrical steel makes it possible to reduce losses in the magnetic core from 580 W to 190 W. The influence of rotation speed on air friction losses and the efficiency of the cooling system is analyzed in detail. However, the work does not pay enough attention to the issues of optimizing cooling systems for different operating modes.

Our review of the literature [6, 9] shows that current studies on the thermal state and losses in HPPM are aimed at increasing the accuracy of loss calculation, improving methods of thermal analysis, and optimizing cooling systems. At the same time, the issues of mutual consideration of the

influence of the distribution of losses in the structural and active elements of the motor structure and insulation on the temperature regimes and durability of insulating materials remain unresolved. A separate issue, worth investigating in further research, is the assessment and analysis of dynamic processes under variable loads and optimization of structures taking into account the minimization of heating and the maximization of specific weight-dimensional indicators.

The aforementioned allows us to assert that the task of studying the relationship between power losses and motor heating under the influence of uneven distribution of losses and the presence of insulation and structural gaps in HPPMs has not been considered in related literature. That makes it necessary to conduct such a study.

### 3. The aim and objectives of the study

The aim of our work is to establish the relationship between power losses in active structural elements and the temperature state of a small-sized high-speed permanent magnet motor. The results of the study could allow us to substantiate measures to reduce the thermal load on active materials, prolong the service life and resource of trouble-free operation, as well as optimize cooling systems for drives of unmanned aerial vehicles.

To achieve this aim, the following objectives were accomplished:

- to construct a multiphysics finite element field mathematical model of a high-speed permanent magnet motor;
- to determine the thermal state in active structural elements when powered from a source with a sinusoidal voltage at constant and variable rotation speed.

### 4. The study materials and methods

The object of our study is a high-speed permanent magnet motor designed to drive unmanned aerial vehicles and ground robotic systems.

The principal hypothesis of the study assumes the following: the thermal load on the winding insulation and the permanent magnet material is determined by the joint action of losses in various structural elements. At the same time, their relative share varies significantly depending on the rotation frequency and the spectral composition of supply voltage.

The assumptions adopted in the study:

1) the calculation model is built in a two-dimensional statement, which corresponds to the assumption about unlimited axial length and the absence of longitudinal end effects;

2) the thermophysical properties of materials (thermal conductivity, specific heat capacity) are considered independent of temperature within the operating modes studied.

Simplifications accepted in the study:

1) mechanical friction losses in bearings and aerodynamic drag are not taken into account because the subject of the study is electromagnetic processes;

2) analysis is carried out for steady-state operating modes; the influence of transient thermal processes during start-up and dynamic operating modes is beyond the scope of our study.

The mathematical basis of the study is the system of Maxwell's equations in the quasi-stationary approximation,

which is implemented by the finite element method in a two-dimensional statement. The calculation area is limited by the cross-section of the motor under study, taking into account the geometry of the tooth-groove zone of the stator, the shape of the rotor, and permanent magnets. The problem is solved in a non-stationary statement; the time dependence of the vector magnetic potential is calculated with a step that provides the necessary accuracy for taking into account higher harmonics.

The prototype for numerical simulation is a small-sized brushless permanent magnet motor, the design of which is shown in Fig. 1. The outer part of the rotor is made of a solid steel sleeve, on the inner cylindrical surface of which radially magnetized permanent magnets are located. The stator consists of a stacked magnetic core and an armature winding.

To calculate the electromagnetic and thermal fields, a prototype of a small-sized high-speed permanent magnet motor was used, shown in Fig. 1.

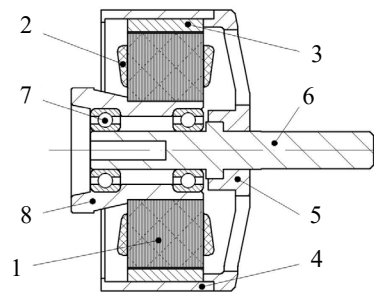


Fig. 1. Sketch of the studied motor: 1 – magnetic core of the stator; 2 – stator winding; 3 – permanent magnets; 4 – rotor sleeve; 5 – rotor “crown”; 6 – shaft; 7 – bearings; 8 – structural stator sleeve

Detailed design and geometric characteristics of the motor under study are given in Table 1.

Table 1  
Basic parameters of the prototype of the motor under study

No.	Parameter	Value
1	Maximum motor power, W	1200.0
2	Rated supply voltage, V	25.0
3	Maximum current, A	54.0
4	Efficiency, %	0.91
5	Number of poles on the rotor	14
8	Axial length, mm	18.0
9	$B_r$ , Tl	1.41
10	Motor outer diameter, mm	45.0
11	Magnetic core material	M530-50A
12	Maximum rotation speed, rpm	23000
13	Air gap, mm	0.15
14	Elemental conductor diameter, mm	0.35
15	Permanent magnet material	N50

Calculations were performed for seven values of rotation speed in the range from 5000 to 23,000 rpm. For each mode, the specific heat release from eddy currents in permanent magnets, losses in the stator magnetic core, and losses in the armature winding were determined. The resulting losses are used as input data for the thermal calculation of the stationary temperature field in the cross section of the motor.

**5. Results of research on the influence of losses in a high-speed electric motor on the thermal state**

**5.1. Multiphysics finite element field mathematical model of a high-speed motor with permanent magnets**

The mathematical basis of the multiphysics model is the well-known system of Maxwell's equations [13] in the quasi-stationary approximation, which is used for electric machines, in which the size of the active zone is smaller than the length of the electromagnetic wave at the operating frequency. The electromagnetic problem is solved relative to the vector magnetic potential, the equation for determining which takes the following form

$$\nabla \times (\nu \nabla \times \mathbf{A}) + \sigma \frac{\partial \mathbf{A}}{\partial t} = \mathbf{J}_s + \nabla \times (\nu \mathbf{B}_r), \tag{1}$$

where  $\nu = 1 / \mu$  – magnetic resistance of the material, m/H;  $\sigma$  – specific electrical conductivity, S/m;  $\mathbf{J}_s$  – vector of external current density in the conductors of the armature winding, A/m<sup>2</sup>;  $\mathbf{B}_r$  – vector of residual magnetic induction of permanent magnets, Tl.

The relationship between  $B$  and  $H$  characterizes magnetic properties of the material. For a stacked magnetic core of a stator with a nonlinear magnetization curve, it is given as follows

$$\mathbf{B} = \mu_0 \cdot \mu_r (|\mathbf{H}|) \mathbf{H}, \tag{2}$$

where  $\mu_0$  is the magnetic constant;  $\mu_r(|\mathbf{H}|)$  is the relative magnetic permeability, which is a nonlinear function of the field strength modulus and is given by the magnetization curve of the M530–50A material (Table 1).

When permanent magnets are heated, their properties change. For this purpose, a linear model of demagnetization of permanent magnets is introduced

$$B_r(T) = B_{r0} \cdot [1 + \alpha_{B_r} (T - T_0)], \tag{3}$$

where  $B_{r0}$  is the residual induction at an ambient temperature of 20°C;  $\alpha_{B_r}$  is the temperature coefficient of residual induction for NdFeB N50 class magnets;  $\alpha_{B_r}$  takes a negative value, reflecting the decrease in residual induction upon heating, which is an indicator of thermal demagnetization and changes in the parameters of permanent magnets.

The specific losses in the magnetic core are determined from the generalized Bertotti model [14], which distinguishes three different types of losses in the magnetic core

$$p_{Fe} = k_h f B_m^\alpha + k_e f^2 B_m^2 + k_a f^{1.5} B_m^{1.5}, \tag{4}$$

where  $k_h, k_e, k_a$  – coefficients of hysteresis losses, eddy currents, and additional losses, respectively, determined from the curves of specific material losses;

$f$  – frequency of magnetization reversal;

$B_m$  – amplitude of magnetic induction at any point of the calculation area;

$\alpha$  – exponent for hysteresis losses ( $\alpha \approx 2$  for the selected steel M530–50A).

Accordingly, the total power of losses in the active materials of the calculation area is determined by integrating over the volume

$$P_{Fe} = l_{Fe} \iint_{\Omega_{Fe}} p_{Fe} dA, \tag{5}$$

where  $l_{Fe}$  is the axial length of the magnetic core package (motor);  $\Omega_{Fe}$  is the cross-section of the magnetic core (separate calculation area).

Due to the finite electrical conductivity of the permanent magnet material ( $\sigma \approx 6.25 \cdot 10^5$  Sm/m), eddy currents arise in permanent magnets, which lead to additional losses. The specific power of active losses from eddy currents is described by the following equation

$$P_{pm} = \frac{|\mathbf{J}_e|^2}{\sigma_{pm}} = \sigma_{pm} \left| \frac{dA_z}{dt} \right|^2, \tag{6}$$

where  $\mathbf{J}_e$  – eddy currents in permanent magnets.

For a multi-turn, filled winding with elementary conductors with a diameter of  $d = 0.35$  mm, the specific power loss, taking into account the effect of current displacement and the proximity effect, is described by effective resistivity

$$P_{cu} = p_{cu}(T) \cdot (1 + k_{sk} + k_{pr}) \cdot J_s^2, \tag{7}$$

where  $p_{cu}(T) = \rho_0 [1 + \alpha_{cu} (T - T_0)]$  – specific electrical resistance with temperature dependence  $\alpha_{cu} = 0.00393^\circ\text{C}^{-1}$ ;

$k_{sk}, k_{pr}$  – coefficients of increase in losses from the effect of displacement of currents and the effect of proximity, respectively, which depend on ratio  $d / \delta$ , where  $\delta$  – penetration depth of the electromagnetic field [15].

The stationary temperature field in the cross-section of the motor is described by the equation of heat conduction with distributed heat sources in the following form:

$$\begin{aligned} d_z \rho C_p \mathbf{u} \cdot \nabla T + \nabla \cdot \mathbf{q} &= d_z Q + q_0 + d_z Q_t, \\ \mathbf{q} &= -d_z k \nabla T, \end{aligned} \tag{8}$$

where  $\mathbf{q}$  is the heat flux density vector;  $d_z$  is the axial length of the calculation area;  $\rho$  is the material density of individual elements of the calculation area;  $C_p$  is the specific heat capacity;  $\mathbf{u}$  is the velocity of the medium (convective heat transfer);  $k$  is the thermal conductivity coefficient of each individual material;  $Q$  is the source of losses;  $q_0$  is the surface heat source;  $Q_t$  is the thermoelastic damping.

The presence of the stator winding casing insulation and the effect of the deterioration of thermal conductivity due to the presence of a constructive air gap (for example, epoxy glue) between the magnets and the rotor sleeve affects the distribution of the thermal field. This circumstance is numerically simulated using the equation of the thermal contact layer between the two areas using the appropriate boundary conditions:

$$-\mathbf{n}_d \cdot \mathbf{q}_d = -d_z \frac{(T_u - T_d)}{R_s} + \frac{1}{2} d_z d_s Q_s, \tag{9}$$

$$-\mathbf{n}_u \cdot \mathbf{q}_u = -d_z \frac{(T_d - T_u)}{R_s} + \frac{1}{2} d_z d_s Q_s,$$

where  $\mathbf{n}_d, \mathbf{n}_u$  are the external normals to the lower and upper sides of the layer, which determine the direction of the heat flux through the layer;  $q_d, q_u$  are the heat flux density vectors from the lower and upper surfaces;  $T_u, T_d$  are the temperatures of the upper and lower surfaces at the layer boundary;  $R_s$  is the thermal resistance of the layer;  $d_s$  is the layer thickness (for example, the thickness of the housing insulation or adhesive layer);  $k$  is the effective thermal conductivity of the layer;  $Q_s$  is the heat source inside the layer.

The left-hand side of equation (9) characterizes the heat flux leaving the surface of the region into the layer. The right-hand side consists of two terms responsible for the thermal conductivity through the layer and the heat distribution between the sides of the layer.

The boundary conditions on the outer surface of the stator allow us to model the cooling of the outer surface of the rotor and are given by the convective heat transfer condition in the following form

$$-\lambda \frac{dT}{dn} \Big|_E = h_c (T \Big|_E - T_a), \quad (10)$$

where  $h_c$  is the heat transfer coefficient of the outer surface of the motor;  $T_a$  – ambient temperature;  $n$  is the external normal to the surface.

The multiphysics model predicts the mutual influence of the electromagnetic field on the thermal field and vice versa, which is implemented within the framework of this work and is based on the iterative connection of two problems.

The finite-element model built is characterized by the basic grid parameters: the total number of grid elements is 14,233; the number of boundary elements is 3227; the number of vertices is 213. With such grid parameters, the average time of one calculation is 2 min 40 s.

**5. 2. Determining the thermal state in the active elements of the structure**

The thermal state of a high-speed motor with permanent magnets is determined by the balance between losses and the intensity of their removal to the environment. The sources of heat generation in the motor under study are three different components: losses in the armature winding, losses in the magnetic core, and losses in permanent magnets. These components of losses depend on the supply frequency and the spectral composition of the supply voltage, which causes the unevenness of the thermal field of individual structural elements in different operating modes.

Basically, the heat flux density is concentrated in the winding slots and the magnetic core. It is in these zones that local temperature maxima occur, which negatively affect the insulation of the winding and can lead to irreversible partial demagnetization of permanent magnets during prolonged operation at elevated speeds.

The result of calculating the specific losses in the design area of the motor under study at a rotation speed of 5000 rpm is shown in Fig. 2.

The temperature field distribution inside the design area of the motor under study at a rotation speed of 5000 rpm is shown in Fig. 3.

Inside the motor under study, the temperature distribution is characterized by significant non-uniformity. The temperature distribution of the motor on a line drawn from the center of the rotation axis to a point on the outer surface of the rotor is shown in Fig. 4.

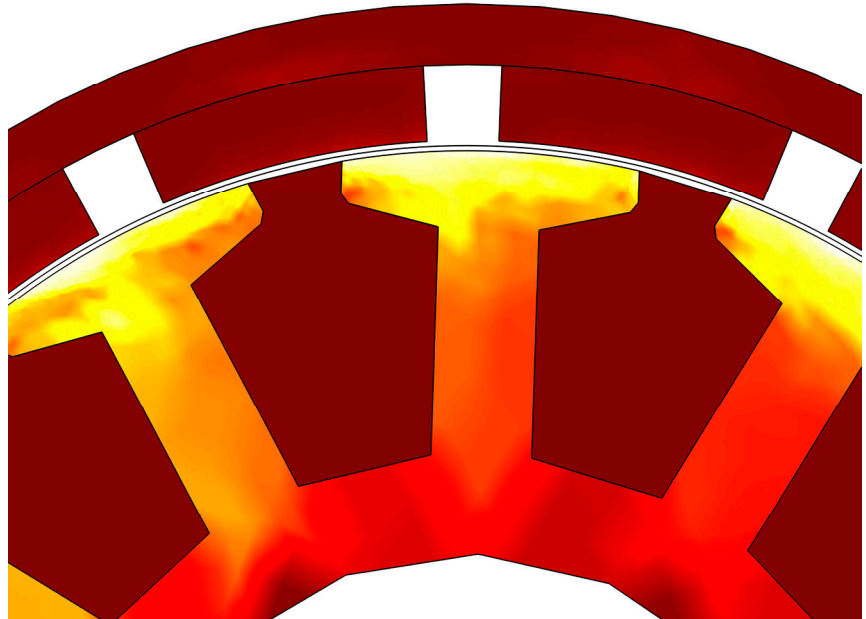


Fig. 2. Result of calculating specific losses

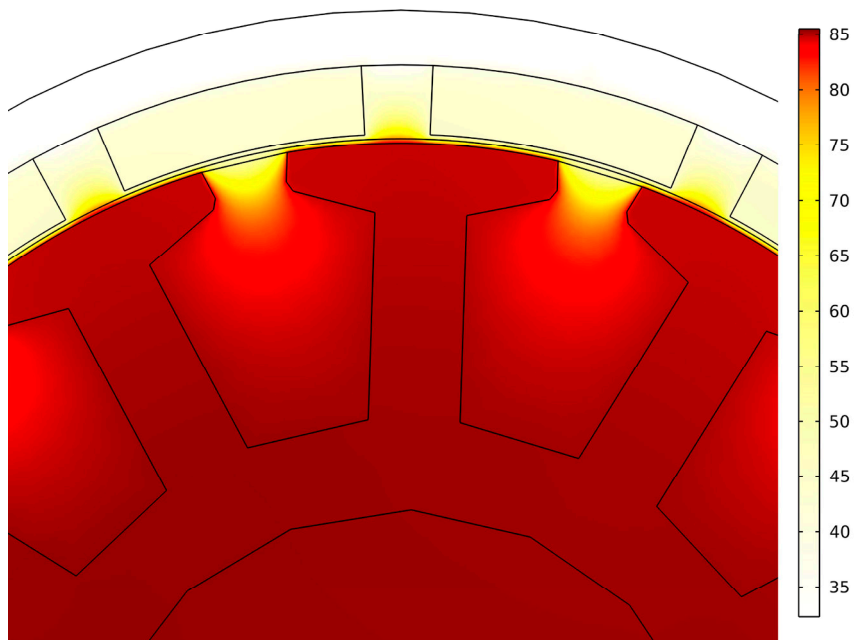


Fig. 3. Temperature field distribution of the motor under study

To assess the impact of losses on the thermal state, a series of calculations were performed, in which the rotation speed was varied at a constant current in the stator winding, which corresponds to a fixed value of the electromagnetic torque. The results of the calculation of motor losses and

average temperature at a low stator winding current of  $\approx 1$  A are given in Table 2.

Table 2

Result of calculation of losses and average temperature

Rotation speed, rpm	Losses, W	Temperature, °C
5000	55.6	55
8000	62.3	63
11000	67.2	69
14000	71.2	74
17000	74.5	79
20000	77.5	83
23000	80.1	87

Electric motors of this design can perform specific technological functions. At the same time, their operation is characterized by a change in torque in a wide range at a constant speed of rotation. The result of calculating the average temperature of the motor at a variable stator current and a constant speed of rotation of 5000 rpm is given in Table 3.

Table 3

Result of calculation of losses and average temperature at 5000 rpm

Stator current, A	Losses, W	Temperature, °C
1	55.6	55
14	69.1	63
27	105.9	87
40	166.0	124
54	256.8	182

The temperature of a brushless permanent magnet motor depends on the magnitude of the electromagnetic torque and the speed of rotation. The dependence of motor temperature on the speed of rotation at different load values is shown in Fig. 5.

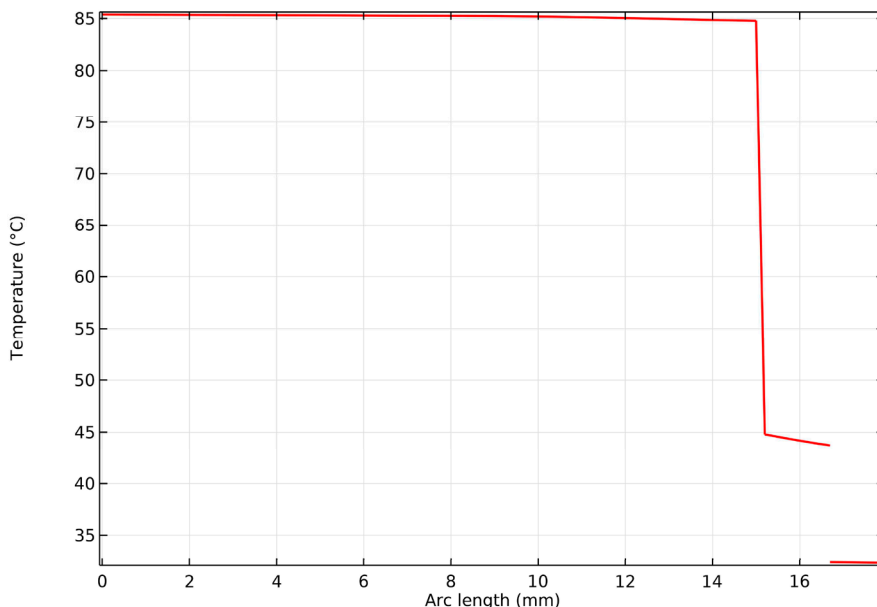


Fig. 4. Temperature distribution of the studied motor in a radial direction

A change in the load (electromagnetic torque) leads to a change in the current in the motor winding and a variable component of losses. The dependence of losses on the current in the armature winding of the studied motor at different speeds of rotation is shown in Fig. 6.

In this way, it is possible to derive the dependence of motor losses and heating from idle mode to maximum load.

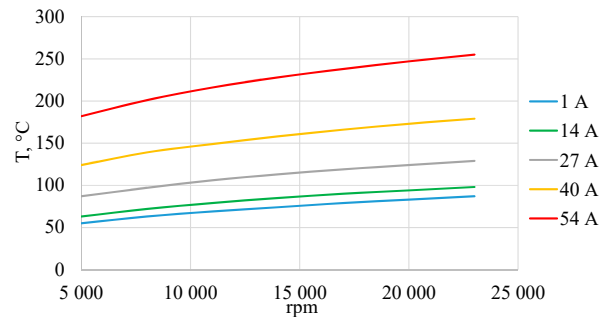


Fig. 5. Dependence of motor temperature on rotation speed at different load values

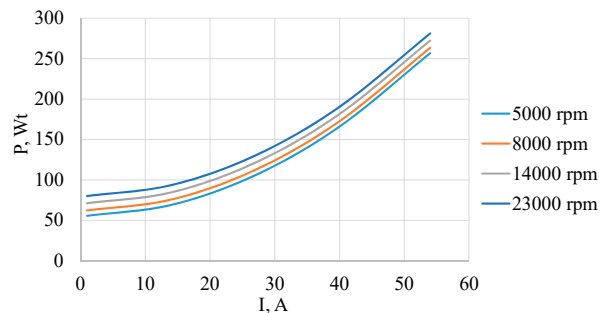


Fig. 6. Dependence of losses on current in the armature winding at different rotation speeds

### 6. Discussion of results based on investigating the influence of losses on the thermal state of a high-speed permanent magnet motor

A multiphysics finite element field mathematical model

of a high-speed permanent magnet motor has been constructed, which takes into account the influence of temperature and losses on the properties of permanent magnet materials. Our results of calculating the temperature distribution in the motor are explained by the physical nature of the heat generation processes in the active elements of the motor structure and the features of their mutual influence when using an interconnected electromagnetic-thermal problem.

With an increase in the rotation speed from 5000 to 23000 rpm, the total magnetic losses increase according to a power law with an index  $\alpha \approx 0.43$  (Fig. 2), which corresponds to the nature of losses in the ferromagnetic stator core. Hysteresis losses increase in proportion to the frequency of magnetization rever-

sal, eddy current losses – in proportion to the square of the frequency. This is confirmed by the nature of temperature field distribution in the cross section (Fig. 3). The maximum heating values are concentrated on the stator teeth, where the losses in the magnetic core are maximum and where the influence of higher harmonics is the greatest, as well as the maximum values of electromagnetic induction. It is these zones that are local temperature maxima (80–85°C) even under the minimum load mode of 1 A, according to the results of thermal calculation.

The pattern of thermal field distribution in the radial direction is characterized by significant non-uniformity (Fig. 4). In the cross section of the stator magnetic core, the temperature is  $\approx 75\text{--}85^\circ\text{C}$ , which corresponds to the zone of the most intense heat generation in the active part of the motor (stator winding and magnetic core). Then there is a sharp drop in temperature to the level of  $\approx 45^\circ\text{C}$ , which indicates the transition of the heat flux through the interface of materials with high thermal resistance – the air gap. A sharp temperature drop at this boundary indicates that the main heat is retained in the active zone. For high-speed motors, this determines the important role of the need for cooling and the need to take into account the thermal expansion of materials in the air gap zone. The final temperature decrease to  $32^\circ\text{C}$  means the boundary of the outer surface of the rotor and the environment, where the temperature is assumed to be  $25^\circ\text{C}$ .

At constant current and torque values (Table 2), the change in motor temperature is due to the dependence of losses on rotor speed. With an increase in speed from 5000 to 23000 rpm, an increase in losses from 55.6 W to 80.1 W is observed, which leads to an increase in average heating from  $55^\circ\text{C}$  to  $87^\circ\text{C}$ . This is explained by an increase in magnetic losses in the ferromagnetic core of the stator (an increase in the frequency of magnetization reversal) due to an increase in the frequency of the supply voltage. The limitation of the temperature increase by an average of  $5\text{--}8^\circ\text{C}$  with an increase in speed in increments of 3,000 rpm is due to the intensification of cooling of the outer casing of the motor.

The increase in motor heating at constant speed and variable load torque (Table 3) is due to the increase in active losses in the stator winding. An increase in the stator current above the rated value of  $\approx 35\text{ A}$  leads to an excessive increase in the average motor temperature  $> 120^\circ\text{C}$ , which is a practical limit for class “F” insulation. Motor operation at maximum power of 1200 W leads to a critical increase in the motor temperature of  $\approx 182^\circ\text{C}$  even when using more heat-resistant class “C” insulation. The main danger of motor operation at maximum power is associated with the risk of thermal damage to permanent magnets and deterioration of motor characteristics. The relationship between temperature and the residual induction of permanent magnets causes the nonlinear behavior  $B_r$ . When the magnets are heated above  $80^\circ\text{C}$  (at current  $> 40\text{ A}$ , at any speed), the  $B_r$  value decreases by 6–8%, which leads to a change in the magnetic flux and a decrease in the electromagnetic torque of  $\approx 3\text{--}4\%$ .

The most dangerous mode of operation of the studied motor is operation at maximum torque (at 54 A) regardless of the speed of rotation (Fig. 5). In this case, the average temperature of the motor changes from  $182^\circ\text{C}$  at 5000 rpm to  $255^\circ\text{C}$  at 23000 rpm. Despite the improvement of cooling conditions with an increase in the speed of rotation from 5000 rpm to 23000 rpm, the temperature of permanent magnets at maximum power changes from  $103^\circ\text{C}$  to  $140^\circ\text{C}$ . Long-term

operation at such power can lead to irreversible partial loss of magnetic properties; therefore, long-term operation of the motor at currents  $> 40\text{ A}$  must be limited.

It was found that the heating is affected by the motor operating mode and rotation speed (Fig. 6). At low loads, magnetic losses prevail, which increase with increasing speed from  $\approx 50\text{ W}$  at 5000 rpm to  $\approx 80\text{ W}$  at 23000 rpm, which is a difference of  $\approx 45\%$ . This corresponds to the power law of the increase in magnetization reversal losses and eddy currents with frequency. With increasing current, all curves have a parabolic character, which is determined by losses in the stator winding. Already at  $I = 27\text{ A}$ , copper losses ( $\sim 50\text{ W}$ ) become commensurate with magnetic losses, and at a maximum current of 54 A they are more than 200 W and dominate the thermal balance. A feature is that with increasing current, the curves for different speeds gradually coincide: at  $I = 54\text{ A}$ , the difference between 5000 and 23000 rpm is only  $\approx 20\text{ W}$  ( $\approx 7\%$  of the total losses of 260–280 W). That is, at high loads, the thermal state of the motor is determined by losses in the winding. Therefore, the cooling efficiency under maximum, and close to them, operating modes should be evaluated primarily by the ability to remove heat from the armature winding.

Compared with similar studies [2, 5], this work takes into account the mutual influence of electromagnetic parameters on thermal parameters and vice versa.

The advantage of the proposed approach is the ability to obtain a picture of the thermal state of permanent magnets in the cross section of the motor under study. This is a practically important result for the design of drives for unmanned aerial vehicles, where the temperature degradation of magnets is a determining factor in the resource and reliability of operation.

The limitations of our study are related to the implementation of the model in a two-dimensional statement, which means the absence of the influence of end effects and a uniform distribution of the field along the motor axis. The contact thermal resistance between the magnets and the rotor, as well as between the winding and the stator slot in the model is taken into account by boundary conditions, which could lead to an underestimation of local temperature maxima in the corresponding zones.

The disadvantages of the study include the lack of consideration of the degradation of the thermophysical properties of materials with temperature, which overestimates the calculated efficiency of heat removal from the winding. In addition, the model does not take into account the cyclic nature of the UAV drive load, in which the determining factor of the resource is not constant but the maximum instantaneous temperature under transient modes.

Future studies may investigate the transition to a three-dimensional statement of the problem in order to take into account end effects and additional losses from uneven temperature distribution along the motor axis. It is also promising to supplement the model with a non-stationary thermal module for analyzing transient temperature regimes.

---

## 7. Conclusions

---

1. A multiphysics numerical finite-element model of a high-speed motor with permanent magnets in a two-dimensional statement has been built, which resolves the relationship between electromagnetic and thermal processes.

The model constructed takes into account the temperature dependence of residual magnetic induction and specific electrical resistance. Our model makes it possible to obtain the distribution of electromagnetic and thermal fields in individual structural elements depending on the load and rotation speed.

2. The temperature distribution in the cross-section of the motor under study and the quantitative values of the specific power affecting the heat release in the active elements of the motor design have been determined. The research was carried out in the range of rotation speeds of 5000–23000 rpm and current in the stator winding of 1–54 A, which is equivalent to different values of the electromagnetic moment. It was established that the nature of temperature distribution in the active parts of the motor is uneven and the maximum heating values are concentrated on the edges of the stator teeth. As the electromagnetic moment increases, the loss curves for different speeds converge asymptotically: at  $I = 54$  A, the difference in losses is  $\approx 7\%$  of the total losses of 260–280 W. At speeds above 17,000 rpm, the temperature of the magnets exceeds  $80^\circ\text{C}$ , and the decrease in  $B_r$  is more than 6–8% from the rated value of  $B_{r0} = 1.41$  T, which causes a decrease in the electromagnetic moment by  $\approx 3\text{--}4\%$ . The critical average temperature of the motor, at which the temperature of the magnets reaches the risk limit of irreversible demagnetization of  $120^\circ\text{C}$ , is  $\approx 216^\circ\text{C}$ , which corresponds to the mode  $n = 11000$  rpm,  $I = 54$  A. Therefore, it is necessary to limit the long-term operation of the motor under the modes at  $n > 11000$  rpm and the moment corresponding to the peak current of 54 A, or to improve the cooling of the motor, or to choose another brand of permanent magnets.

---

#### Conflicts of interest

The authors declare that they have no conflicts of interest in relation to the current study, including financial, personal, authorship, or any other, that could affect the study and the results reported in this paper.

---

#### Funding

The study was conducted without financial support.

---

#### Data availability

The data will be provided upon reasonable request.

---

#### Use of artificial intelligence

The authors declare that generative artificial intelligence tools were used exclusively for language editing, grammar checking, and technical formatting of the manuscript under full human control.

Artificial intelligence was not used to create, process or interpret scientific data, draw conclusions, or other elements of the scientific results of the manuscript.

Tool used: ChatGPT (OpenAI GPT-5, version 2025).

The authors bear full responsibility for the content, reliability, and scientific correctness of the submitted material.

---

#### Acknowledgments

The work was carried out under the state budget topic No. 2025.06/0044 “Electromechanical systems of increased energy efficiency for aircraft”, funded by the National Research Foundation of Ukraine, 2025–2026.

---

#### Authors' contributions

**Mykhailo Kovalenko:** Writing – original draft, Writing – review & editing, Investigation, Project administration; **Yuriy Gaidenko:** Conceptualization, Supervision; **Serhii Tsyvinskyi:** Validation; **Oleksandr Semenyuk:** Methodology; **Oleh Bazarov:** Resources, Software.

---

#### References

- Ostroverkhov, M., Chumack, V., Falchenko, M., Kovalenko, M. (2022). Development of control algorithms for magnetolectric generator with axial magnetic flux and double stator based on mathematical modeling. *Eastern-European Journal of Enterprise Technologies*, 6 (5 (120)), 6–17. <https://doi.org/10.15587/1729-4061.2022.267265>
- Shen, Q., Zhou, Z., Li, S., Liao, X., Wang, T., He, X., Zhang, J. (2022). Design and Analysis of the High-Speed Permanent Magnet Motors: A Review on the State of the Art. *Machines*, 10 (7), 549. <https://doi.org/10.3390/machines10070549>
- Li, Z., Wang, P., Liu, L., Xu, Q., Che, S., Zhang, L. et al. (2022). Loss calculation and thermal analysis of ultra-high speed permanent magnet motor. *Heliyon*, 8 (11), e11350. <https://doi.org/10.1016/j.heliyon.2022.e11350>
- Gundabattini, E., Mystkowski, A. (2021). Review of air-cooling strategies, combinations and thermal analysis (experimental and analytical) of a permanent magnet synchronous motor. *Proceedings of the Institution of Mechanical Engineers, Part C: Journal of Mechanical Engineering Science*, 236 (1), 655–668. <https://doi.org/10.1177/0954406220987267>
- Meng, T., Zhang, P. (2021). A Review of Thermal Monitoring Techniques for Radial Permanent Magnet Machines. *Machines*, 10 (1), 18. <https://doi.org/10.3390/machines10010018>
- Du, J., Li, C., Zhao, J., Ren, H., Zhang, K., Song, X., Chen, L. et al. (2022). Investigation of Eddy Current Loss and Structure Design with Magnetic-Thermal Coupling for Toothless BLDC High-Speed PM Motor. *Machines*, 10 (2), 118. <https://doi.org/10.3390/machines10020118>
- Dong, J., Huang, Y., Jin, L., Lin, H., Yang, H. (2014). Thermal Optimization of a High-Speed Permanent Magnet Motor. *IEEE Transactions on Magnetics*, 50 (2), 749–752. <https://doi.org/10.1109/tmag.2013.2285017>
- Zhang, M., Luo, S., Liu, X., Li, W. (2021). The eddy current loss segmentation model of permanent magnet for temperature analysis in high-speed permanent magnet motor. *IET Power Electronics*, 14 (4), 751–759. <https://doi.org/10.1049/pel2.12009>

9. Pan, B., Tao, D., Ge, B., Wang, L., Hou, P. (2022). Analysis of Eddy Current Loss of 120-kW High-Speed Permanent Magnet Synchronous Motor. *Machines*, 10 (5), 346. <https://doi.org/10.3390/machines10050346>
10. Yu, Y., Liang, D., Liu, X. (2017). Optimal Design of the Rotor Structure of a HSPMSM Based on Analytic Calculation of Eddy Current Losses. *Energies*, 10 (4), 551. <https://doi.org/10.3390/en10040551>
11. Jumayev, S., Merdzan, M., Boynov, K. O., Paulides, J. J. H., Pyrhonen, J., Lomonova, E. A. (2015). The Effect of PWM on Rotor Eddy-Current Losses in High-Speed Permanent Magnet Machines. *IEEE Transactions on Magnetics*, 51 (11), 1–4. <https://doi.org/10.1109/tmag.2015.2438637>
12. Schmidt, E., Kaltenbacher, M., Wolfschluckner, A. (2017). Eddy current losses in permanent magnets of surface mounted permanent magnet synchronous machines – Analytical calculation and high order finite element analyses. *E & I Elektrotechnik Und Informationstechnik*, 134 (2), 148–155. <https://doi.org/10.1007/s00502-017-0498-y>
13. Kovalenko, M., Tkachuk, I., Kovalenko, I., Zhuk, S., Kryshnov, O. (2024). Double stator axial flux magnetoelectric generator for conversion of low potential mechanical energy. *Vidnovluvana Energetika*, 2 (77), 13–20. [https://doi.org/10.36296/1819-8058.2024.2\(77\).13-20](https://doi.org/10.36296/1819-8058.2024.2(77).13-20)
14. Moradian, K., Sheikholeslami, T. F., Raghebi, M. (2022). Investigation of a spherical pendulum electromagnetic generator for harvesting energy from environmental vibrations and optimization using response surface methodology. *Energy Conversion and Management*, 266, 115824. <https://doi.org/10.1016/j.enconman.2022.115824>
15. Chumack, V., Tsyvinskyi, S., Kovalenko, M., Ponomarev, A., Tkachuk, I. (2020). Mathematical modeling of a synchronous generator with combined excitation. *Eastern-European Journal of Enterprise Technologies*, 1 (5 (103)), 30–36. <https://doi.org/10.15587/1729-4061.2020.193495>